PROCEEDINGS OF SCIENCE

Production of top quarks, jets and photons

Javier Llorente, on behalf of the ATLAS and CMS Collaborations*
Simon Fraser University
E-mail: javier.llorente.merino@cern.ch

Measurements of the production of top quarks, jets and photons using the ATLAS and CMS detectors at the LHC are presented. Top quark results include the measurement of highly boosted $t\bar{t}$ pairs decaying exclusively to hadrons as well as differential cross sections in various decay channels which are, in some cases, used to determine the strong coupling constant and the mass of the top quark. Measurements of jet production probe both the perturbative and non-perturbative regime, including measurements of dijet and trijet production in the back-to-back limit as well as fragmentation, gluon splitting and event shape studies. Photon analyses include measurements of the inclusive photon and photon plus jet cross sections, as well as the ratio of the cross sections for the centre-of-mass energies of 13 TeV and 8 TeV.

7th Annual Conference on Large Hadron Collider Physics - LHCP2019
20-25 May, 2019
Puebla, Mexico

*Speaker.

PoS(LHCP2019)087

Quantum Chromodynamics (QCD) is the theory describing the strong interaction between coloured objects, namely quarks and gluons, which compose the colourless hadronic matter. This note briefly describes several measurements probing QCD using various objects, including top quarks, jets and photons, using data obtained with the ATLAS [1] and CMS [2] detectors at the Large Hadron Collider. These results are interpreted in terms of perturbative QCD (pQCD) and non-perturbative QCD (npQCD) by comparing the data with fixed-order theoretical predictions in pQCD as well as with Monte Carlo (MC) simulations modelling different aspects of these physics processes, such as parton showers or fragmentation functions. Some of the results involving top quarks are then used to determine various parameters of the QCD Lagrangian, such as the strong coupling constant α_s and the top quark mass m_t.

1. Measurements of top quark production

The cross sections of top quark pair production have been measured in a wide variety of final states, including topologies in which the top quark is boosted, produced in association with additional jets and in different decay channels of the W bosons arising from the top decay.

The ATLAS Collaboration has recently presented a measurement of the differential cross section of boosted, hadronically decaying top quark pairs in Ref. [3]. The selection criteria include two jets, clustered with the anti-k_t algorithm [4], with a radius parameter of $R = 1.0$ and whose transverse momenta fulfill $p_T > 350$ GeV. The jet mass is required to differ from the top mass by less than 50 GeV, and each of these jets has to be associated with a b-tagged jet within a distance $\Delta R = \sqrt{(\Delta\eta)^2 + (\Delta\phi)^2} < 1.0$. These jets are then considered as reconstructed top quarks, and several kinematic variables of the $t\bar{t}$ system are measured and compared to MC predictions. Another recent ATLAS analysis [5] presents a measurement of $t\bar{t}$ production in association with additional jets. In this case, events are selected in the lepton+jets channel by requiring one electron or muon with $p_T > 25$ GeV and $|\eta| < 2.5$. All jets with radius parameter $R = 0.4$, $p_T > 25$ GeV and $|\eta| < 2.5$ are preselected, and kinematic variables of the $t\bar{t}$+jets system are studied. Figure 1 shows the distributions of the transverse momentum of the $t\bar{t}$ system for two different topologies: the boosted case in Ref. [3] and the six jet inclusive topology in Ref. [5]. Results are compared to fixed order QCD predictions by POWHEG [6] and MG5_aMC@NLO [7] matched to PYTHIA [8] or HERWIG [9] parton showers. Predictions by SHERPA [10] are also shown.

The CMS Collaboration has presented measurements of differential cross sections of the production of top pairs in the dileptonic channel, where both W bosons decay into a charged lepton and a neutrino [11, 12, 13]. These data have also been used to determine physical constants such as the strong coupling constant α_s and the top quark mass m_t, and also to constrain the parton distribution functions (PDF). In Ref. [11], events are selected by requiring two isolated, charged leptons (electron or muon) with $p_T > 25$ (20) GeV for the leading (subleading) lepton, together with $R = 0.4$ jets with $p_T > 30$ GeV. Using the comparison of various distributions in data to next-to-next-to-leading order (NNLO) predictions in pQCD, the values of the strong coupling constant and the top mass in the $\overline{\text{MS}}$ scheme are determined by means of χ^2 fits. The values of these parameters are summarised in Table 1 for different PDF sets. Reference [12] presents the $t\bar{t}$ differential

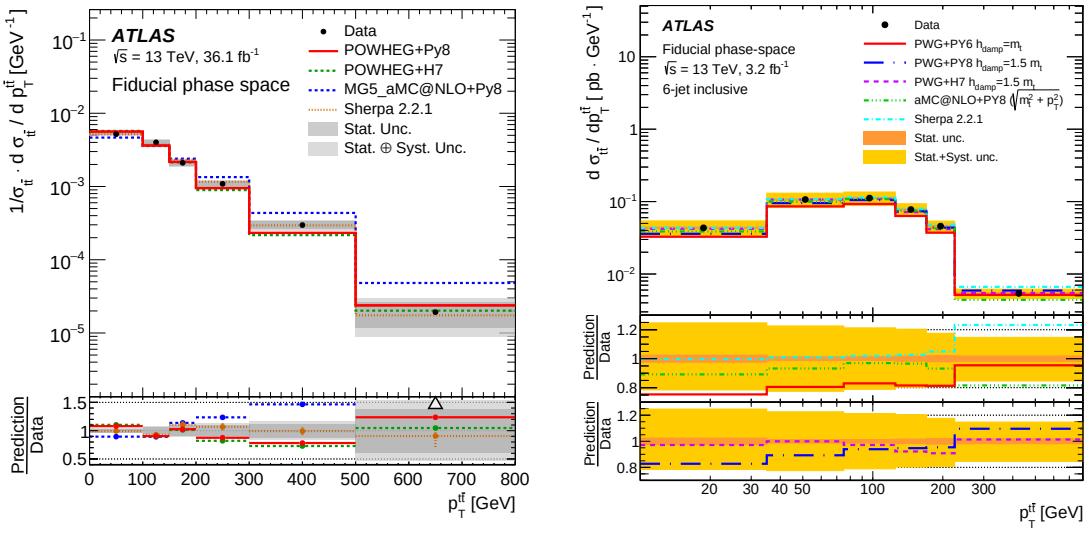

Figure 1: Transverse momentum distribution of the $t\bar{t}$ system in boosted, hadronically decaying topologies (left) [3] and in six jet inclusive topologies in the lepton+jets channel (right) [5]

PDF set	$\alpha_s(m_Z)$	$m_t(m_t)$ [GeV]
ABMP16	0.1139 ± 0.0023 (fit+PDF)$^{+0.0014}_{-0.0001}$ (scale)	161.6 ± 1.6 (fit+PDF+α_s)$^{+0.1}_{-1.0}$ (scale)
NNPDF3.1	0.1140 ± 0.0033 (fit+PDF)$^{+0.0021}_{-0.0002}$ (scale)	164.5 ± 1.6 (fit+PDF+α_s)$^{+0.1}_{-1.0}$ (scale)
CT14	0.1148 ± 0.0032 (fit+PDF)$^{+0.0018}_{-0.0002}$ (scale)	165.0 ± 1.8 (fit+PDF+α_s)$^{+0.1}_{-1.0}$ (scale)
MMHT14	0.1151 ± 0.0035 (fit+PDF)$^{+0.0020}_{-0.0002}$ (scale)	164.9 ± 1.8 (fit+PDF+α_s)$^{+0.1}_{-1.1}$ (scale)

Table 1: Values of the strong coupling constant $\alpha_s(m_Z)$ and the top mass $m_t(m_t)$ in the $\overline{\text{MS}}$ scheme, determined from CMS data [11]

cross sections are measured by CMS as a function of basic kinematic observables for each of the top quarks. They are compared to several theoretical predictions including full NNLO predictions matched next-to-next-to-leading logarithmic (NNLL) resummation of soft gluon terms as well as electroweak corrections up to orders $\mathcal{O}(\alpha^3_{\text{EW}})$. Fig. 2 shows the comparison of the differential cross sections as a function of the top quark p_T, corrected up to hadron and parton levels, with theoretical predictions at different perturbative and resummation orders.

In Ref. [13], the CMS Collaboration presents multi-differential cross section measurements as a function of various kinematic variables. This includes a triple-differential measurement as a function of the invariant mass and rapidity of the $t\bar{t}$ pair as well as the multiplicity of additional jets. Figure 3 presents the double differential cross section as a function of the p_T of the $t\bar{t}$ system and its invariant mass. These measurements are used to determine the value of the strong coupling constant α_s and the top quark pole mass m_t^{pole} in a simultaneous fit together with the PDFs by comparing the data to NLO predictions, yielding:

$$\alpha_s(m_Z) = 0.1135 \pm 0.0016\ (\text{fit})\ ^{+0.0002}_{-0.0004}\ (\text{mod.})\ ^{+0.0008}_{-0.0001}\ (\text{par.})\ ^{+0.0011}_{-0.0005}\ (\text{scale}) \tag{1.1}$$

$$m_t^{\text{pole}} = 170.5 \pm 0.7\ (\text{fit})\ \pm 0.1\ (\text{mod.})\ ^{+0.0}_{-0.1}\ (\text{par.})\ \pm 0.3\ (\text{scale}) \tag{1.2}$$

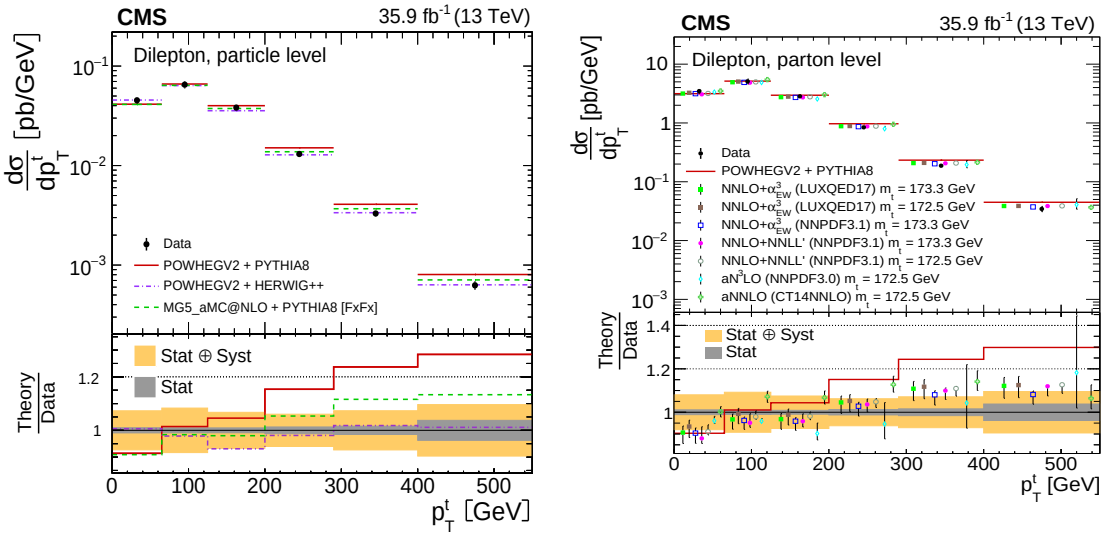

Figure 2: Differential cross section as a function of the top quark p_T at particle (left) and parton level (right), compared to theoretical predictions [12]

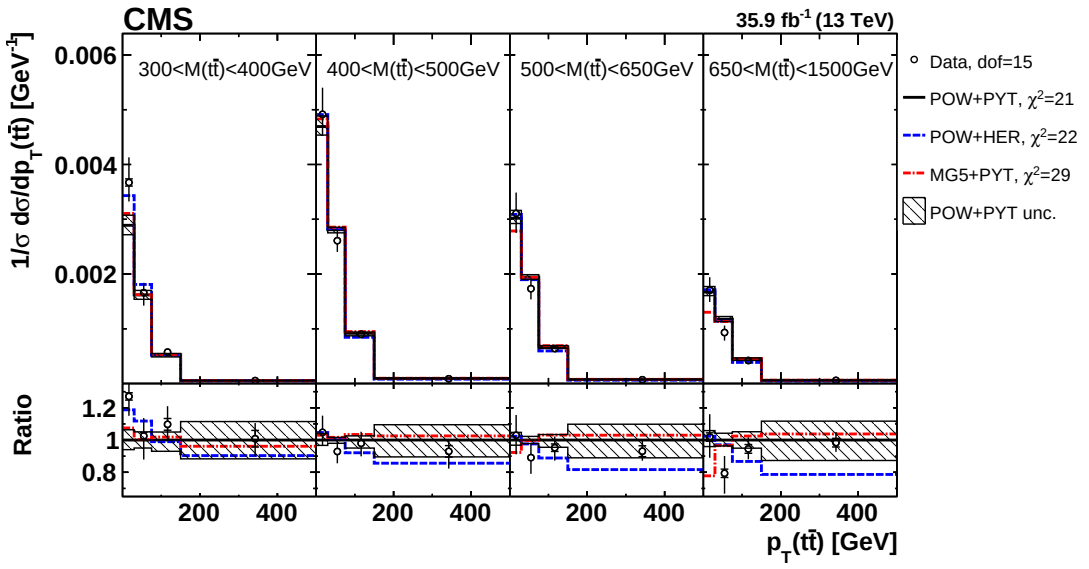

Figure 3: Double-differential cross section of $t\bar{t}$ pairs as a function of the transverse momentum, in bins of invariant mass of the $t\bar{t}$ system, compared to NLO theoretical predictions matched to parton showers [13].

2. Measurements of jet production

Multijet events are a natural environment to test QCD in multiple regimes. Studies on the topology of multijet events are usually sensitive to aspects of perturbative QCD and the resummation procedure, while jet substructure measurements are typically used as a means to probe the different hadronization models.

Fragmentation functions $D^h_{q,g}(z,Q)$ parameterise the probability of a parton, quark or gluon, with an energy scale Q to produce a hadron h with a momentum fraction z with respect to the energy of the original parton. Recently, the ATLAS Collaboration has published a measurement of jet fragmentation using charged particles in dijet events [14]. In this analysis, several observables sensitive to the jet fragmentation functions are measured, including the multiplicity of charged particles $\langle n_{\mathrm{ch}}$, the momentum fraction $\zeta = p_{\mathrm{T}}^{\mathrm{part}}/p_{\mathrm{T}}^{\mathrm{jet}}$, the transverse profile $p_{\mathrm{T}}^{\mathrm{rel}} = p_{\mathrm{T}}^{\mathrm{part}} \sin\theta_{jp}$ or the radial profile, given by the number of charged particles at a distance r from the jet axis. These data are used to extract separate quark and gluon distributions making use of the fact that, for a given p_{T}, the probability of a jet being initiated by a quark or a gluon depends on the pseudoraridity, i.e. quarks are favoured in the forward direction. The quark and gluon distributions are obtained using two different methods, by means of a simple linear system of equations or using a model-independent approach known as 'Topic modelling' [15]. For bin i of a given distribution, the first and second Topics can be expressed as a function of the distributions for the most central (c) and forward jets (f) as:

$$h_i^{T_1} = \frac{h_i^f - \min_j\{h_j^f/h_j^c\} \times h_i^c}{1 - \min_j\{h_j^f/h_j^c\}}; \quad h_i^{T_2} = \frac{h_i^c - \min_j\{h_j^c/h_j^f\} \times h_i^f}{1 - \min_j\{h_j^c/h_j^f\}} \tag{2.1}$$

Where Topic 1 defines a quark-enriched sample and Topic 2 defines the gluon-like sample. Figure 4 shows the average number of charged particles as a function of the jet p_{T} for all selected jets, compared to MC expectations; as well as for both Topics defined in Eq. 2.1.

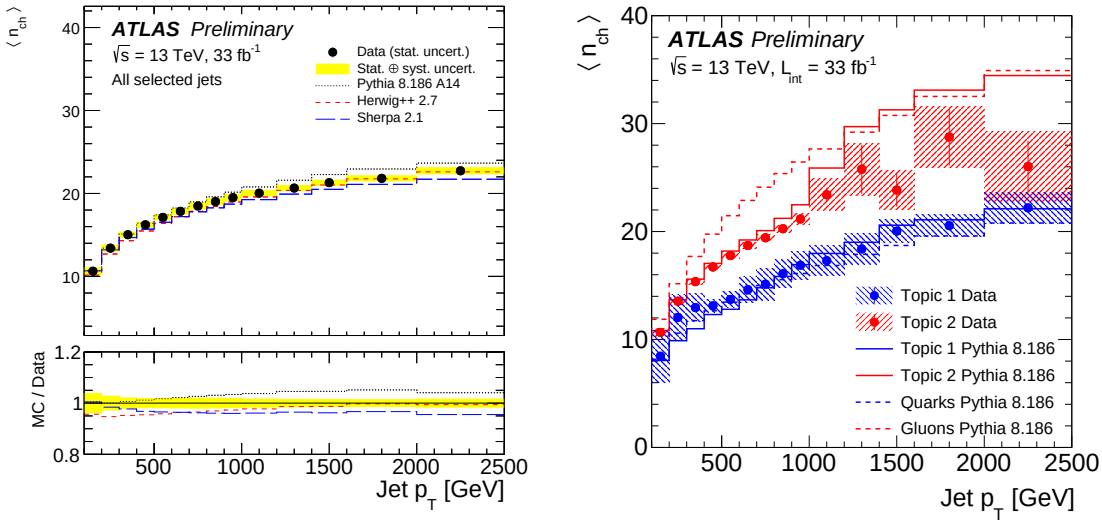

Figure 4: Average number of charged particles as a function of the jet p_{T} for all selected jets (left) and topics T_1 and T_2 compared to quark and gluon-like jets (right) [14]

The results show a good agreement between Topic 1 and quark-like jets in MC, while significant discrepancies are observed between Topic 2 and gluon-like jets in MC.

A study of the gluon splitting $g \to b\bar{b}$ has been recently presented by the ATLAS Collaboration in Ref. [16]. In order to reconstruct this final state, jets with a large radius parameter of $R = 1.0$ are clustered using the anti-k_t algorithm. These jets are considered as a reconstructed proxy for the gluon four-momentum, while the b-quark jets are reconstructed as two anti-k_t jets with a smaller radius of $R = 0.2$, using charged particles as inputs. Small radius jets are then associated with large radius jets by means of ghost association [17], and observables such as the angular distance $\Delta R_{b\bar{b}}$, the momentum sharing $z = p_{\mathrm{T}2}/(p_{\mathrm{T}1} + p_{\mathrm{T}2})$ or the angle between the production and decay planes of the gluon, $\theta_{ppg,gbb}$, which carries the information about the gluon polarization, are measured. In order to determine the purity of $g \to b\bar{b}$ decays in the selected sample, likelihood fits are performed to the signed impact parameter of the tracks used to reconstruct both b-jets, and the distributions are corrected using the determined flavour fractions for $b\bar{b}$ pairs. Figure 5 shows the flavour fraction in Monte Carlo before and after the likelihood fits as a function of the angle between the gluon production and decay planes, $\theta_{ppg,gbb}$ as well as the distribution of $\theta_{ppg,gbb}$ compared to different Monte Carlo predictions. These results show differences between Monte Carlo and data for the distribution of $\theta_{ppg,gbb}$, with PYTHIA [8] showing larger discrepancies than SHERPA [10]. In any case, the data favour a lesser degree of polarization than expected from MC models.

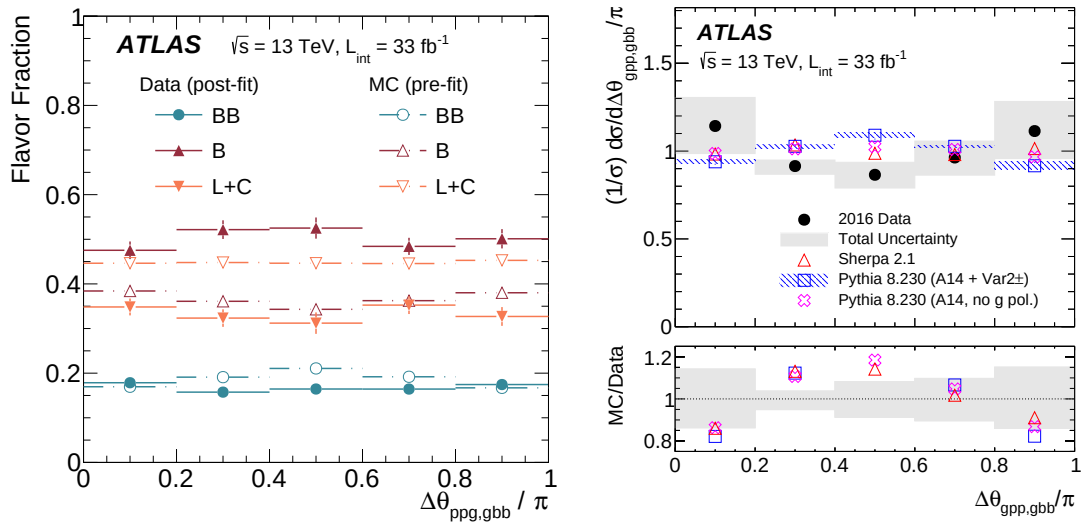

Figure 5: Flavour fraction for jets in MC simulation before and after the likelihood fit as a function of $\theta_{ppg,gbb}$ (left), and the distribution of $\theta_{ppg,gbb}$ compared to MC expectations [16].

In Ref. [18], the CMS Collaboration presents a study of event shapes in multijet final states. These sets of observables are a measure of the homogeneity and isotropy of the energy distribution in the space. The so-called thrust axis is determined as the direction of space that maximizes the energy projection of all jets in the event. The transverse thrust is defined as

$$\tau_{\perp} = 1 - \max_{\hat{n}_T} \frac{\sum_i |\vec{p}_{Ti} \cdot \hat{n}_T|}{\sum_i p_{\mathrm{T}i}} \tag{2.2}$$

The thrust axis $\hat{n}_T$ divides the space in two hemispheres U and L by considering the jets for which the quantity $\vec{p}_{Ti} \cdot \hat{n}_T$ is positive (U) or negative (L). Then, the directions of all jets in each hemisphere X are averaged by defining the hemisphere coordinates

$$\eta_X = \frac{\sum_{i \in X} p_{\mathrm{T}i} \eta_i}{\sum_{i \in X} p_{\mathrm{T}i}}; \quad \phi_X = \frac{\sum_{i \in X} p_{\mathrm{T}i} \phi_i}{\sum_{i \in X} p_{\mathrm{T}i}}, \tag{2.3}$$

and the jet broadening for hemisphere X is defined as

$$B_X = \frac{1}{2P_{\mathrm{T}}} \sum_{i \in X} p_{\mathrm{T}i} \sqrt{(\eta_i - \eta_X)^2 + (\phi_i - \phi_X)^2}. \tag{2.4}$$

The total jet broadening is then defined as the sum of the jet broadening for each hemisphere, $B_{\mathrm{tot}} = B_U + B_L$. Figure 6 shows the distribution of the logarithm of the transverse thrust defined in Eq. 2.2, as well as the logarithm of the total jet broadening B_{tot} compared to expectations from different parton shower Monte Carlo models.

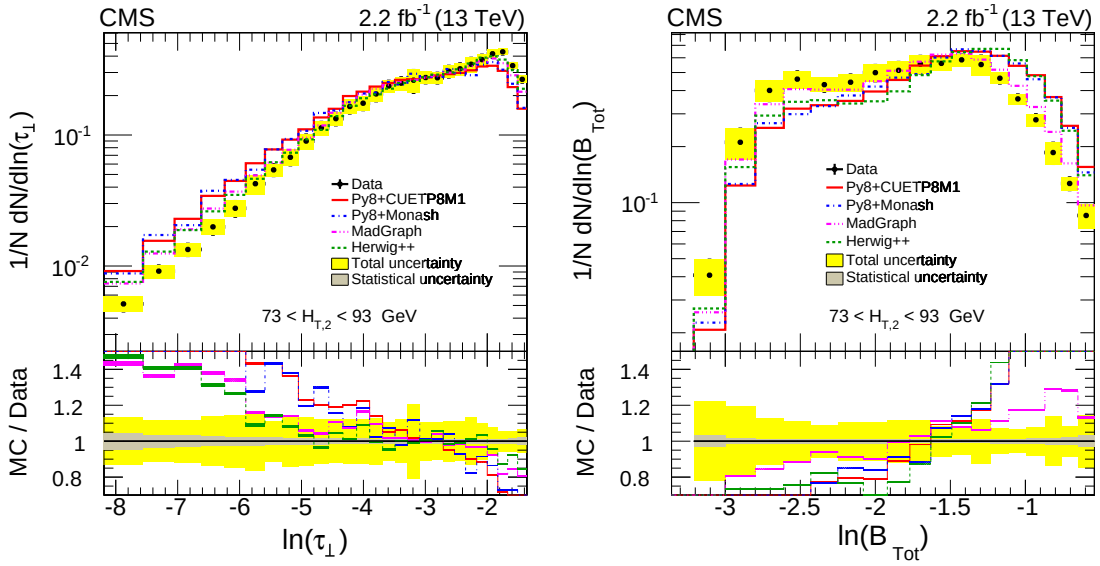

Figure 6: Distributions of the logarithms of the transverse thrust $\tau_\perp$ (left) and the total jet broadening B_{tot} (right) compared to different Monte Carlo expectations [18].

In general, none of the Monte Carlo models investigated gives a good description of the data for the event shape distributions. This observation applies especially to the lower tail of the distributions, where the resummation effects are large.

Another test of parton showers and resummation effects in multijet topologies is presented in Ref. [19]. Here, the distribution of the azimuthal difference $\Delta\phi_{12}$ between the two leading jets is measured in the nearly back-to-back region, $\Delta\phi_{12} \lesssim \pi$, for two event selection categories. First, dijet events are selected by considering events with at least two jets with $p_{\mathrm{T}} > 100$ GeV. Second, a third jet with $p_{\mathrm{T}} > 30$ GeV is required. Due to the azimuthal decorrelation, the $\Delta\phi_{12}$ distribution is flatter in the case of three-jet events, while it peaks sharply at values close to π for the dijet selection.

Figure 7 shows the results for the $\Delta\phi$ distribution in both selections, together with MC expectations by PYTHIA and HERWIG++ [9].

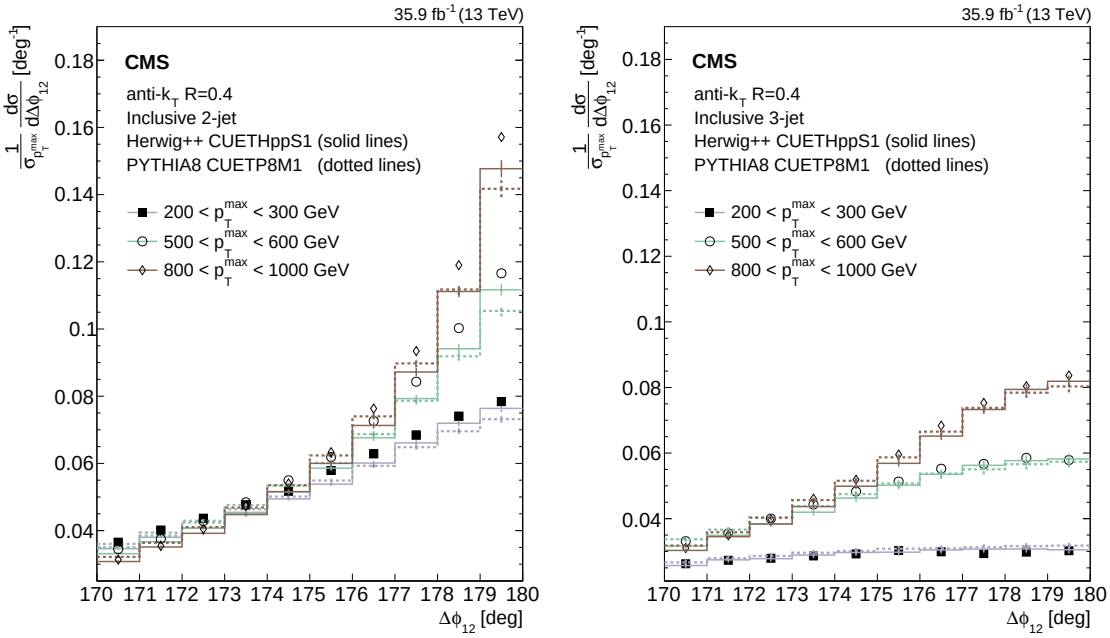

Figure 7: Distributions of the azimuthal difference $\Delta\phi_{12}$ between the two leading jets for two-jet (left) and three-jet events (right) [19].

Additionally, comparisons to NLO predictions by POWHEG [6] in which the $2 \to 2$ and $2 \to 3$ matrix elements are matched to parton showers by PYTHIA and HERWIG++ are presented. It is observed that the two-jet and three-jet measurements are not simultaneously described by any of these models.

3. Measurements of photon production

Measurements of the kinematic properties of isolated photons constitute precision tests of QCD using a colourless object. In particular, measurements of the production cross section of inclusive photons can be compared to fixed-order pQCD predictions to evaluate the description provided by the theory, for which NNLO corrections have been recently included [20].

The scale evolution of the photon production cross section can be tested by considering the ratio of the differential distributions at different values of the centre-of-mass energy of the incoming protons. Recently, the ATLAS Collaboration has published the measurement of this ratio, $R^{\gamma}_{13/8}$, [21] for values of the centre-of-mass energy of $\sqrt{s} = 13$ TeV [22] and $\sqrt{s} = 8$ TeV [23]. The proper treatment of the correlations between the experimental and theoretical uncertainties for both measurements provides a drastic reduction of the total uncertainty on the ratio, compared to the non-correlation hypothesis. The left panel in Fig. 8 illustrates this reduction for the experimental uncertainties. For the theoretical uncertainties shown in the right-hand-side of Fig. 8, a coherent treatment for the variation of renormalization and factorization scales in both measurements leads to a total scale uncertainty of $\mathcal{O}(2\%)$, whereas an incoherent treatment of the scale variations would lead to an overestimated uncertainty of $\mathcal{O}(14\%)$.

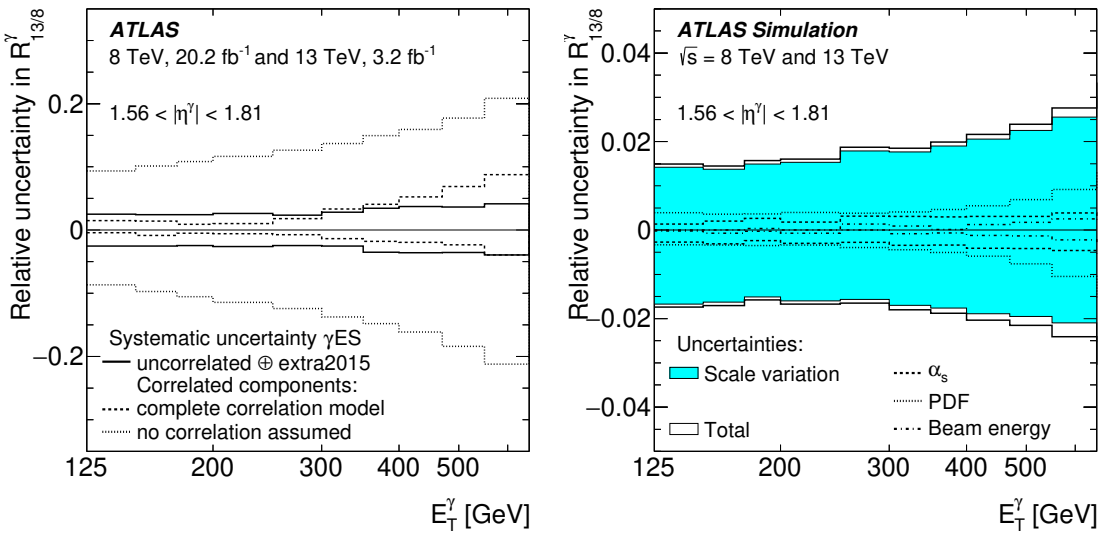

Figure 8: Experimental (left) and theoretical uncertainties (right) for the ratio of inclusive photon cross sections at $\sqrt{s} = 13$ TeV and $\sqrt{s} = 8$ TeV [21]. A large reduction of the uncertainties is achieved by properly treating the correlations between the uncertainties in both measurements.

In order to achieve a further reduction of the experimental uncertainties, the double ratio $D^{\gamma}_{13/8} = R^{\gamma}_{13/8}/R^{Z}_{13/8}$ is considered, where $R^{Z}_{13/8}$ is the ratio of the total integrated cross sections for Z boson production at $\sqrt{s} = 13$ TeV and $\sqrt{s} = 8$ TeV. In this way, the uncertainty due to the luminosity measurement for both centre-of-mass energies is cancelled and thus the total uncertainty is reduced. Figure 9 shows the comparison of the ratios $R^{\gamma}_{13/8}$ and $D^{\gamma}_{13/8}$ for $|\eta^{\gamma}| < 0.6$ with the theoretical predictions in pQCD at the highest available order. The inclusive photon differential

cross sections are calculated at NLO, while the total cross sections for Z production are computed at NNLO.

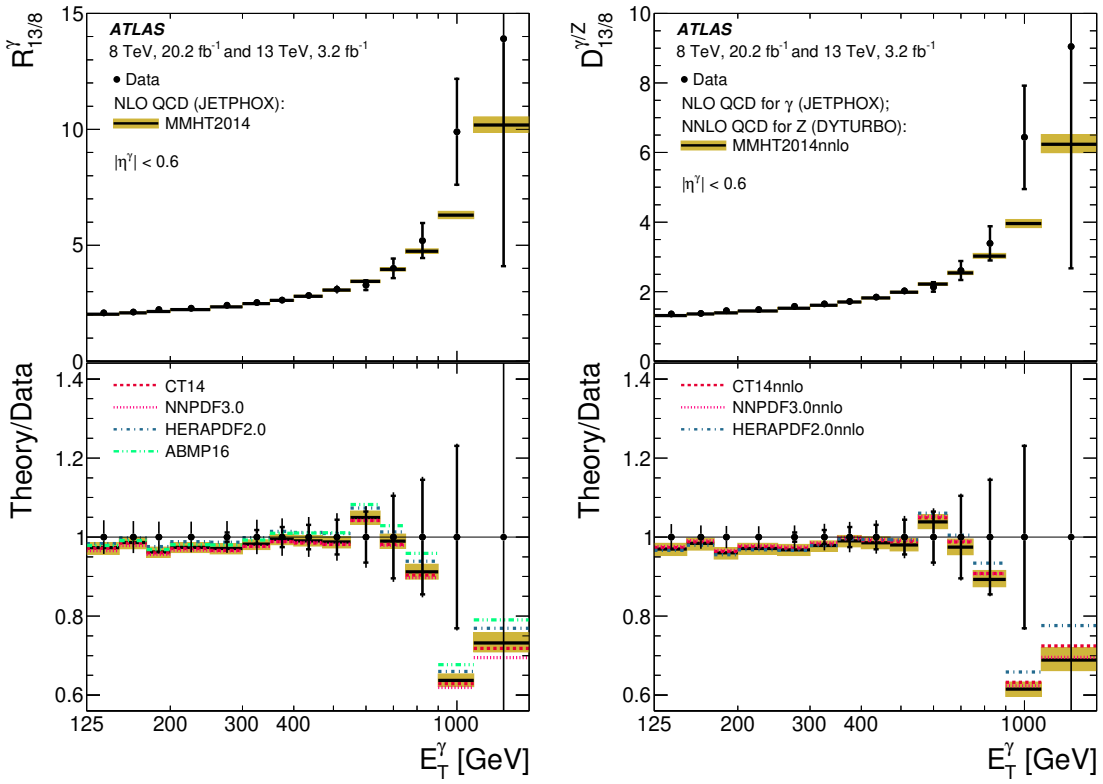

Figure 9: Ratio $R^{\gamma}_{13/8}$ of the inclusive photon differential cross section as a function of E^{γ}_{T} at centre-of-mass energies $\sqrt{s} = 13$ TeV and $\sqrt{s} = 8$ TeV for $|\eta^{\gamma}| < 0.6$ (left). Double ratio $D^{\gamma}_{13/8}$ of $R^{\gamma}_{13/8}$ for $|\eta^{\gamma}| < 0.6$ to the total Z boson production cross section ratio $R^{Z}_{13/8}$ (right) [21]

The inclusive photon and photon plus jet cross sections have also been measured by the CMS Collaboration in Ref. [24]. These measurements require an isolated photon with transverse energy above 190 GeV and $|y| < 2.5$. Furthermore, for the γ+jet measurement, at least an additional jet with $p_T > 30$ GeV and $|y| < 2.4$ is required. In order to discriminate from the misidentified photon background, mainly from multijet production, a Boosted Decision Tree is trained and validated using the sideband regions of the photon isolation distribution. The cross section for inclusive photon production is presented as a function of the transverse energy of the photon, E^{γ}_{T}, and its rapidity y^{γ}. For the γ+jet case, results are given as a function of E^{γ}_{T}, y^{γ} and the rapidity of the jet y^{jet}. Figure 10 shows the results for both measurements, compared to NLO QCD predictions by JETPHOX [25, 26, 27]. A more detailed comparison of the data and theoretical predictions is shown in Fig. 11, where the ratios of the theoretical predictions to the data are presented together with the experimental and theoretical uncertainties. The agreement between theory and data is good, within the uncertainties, for all the phase space regions under study.

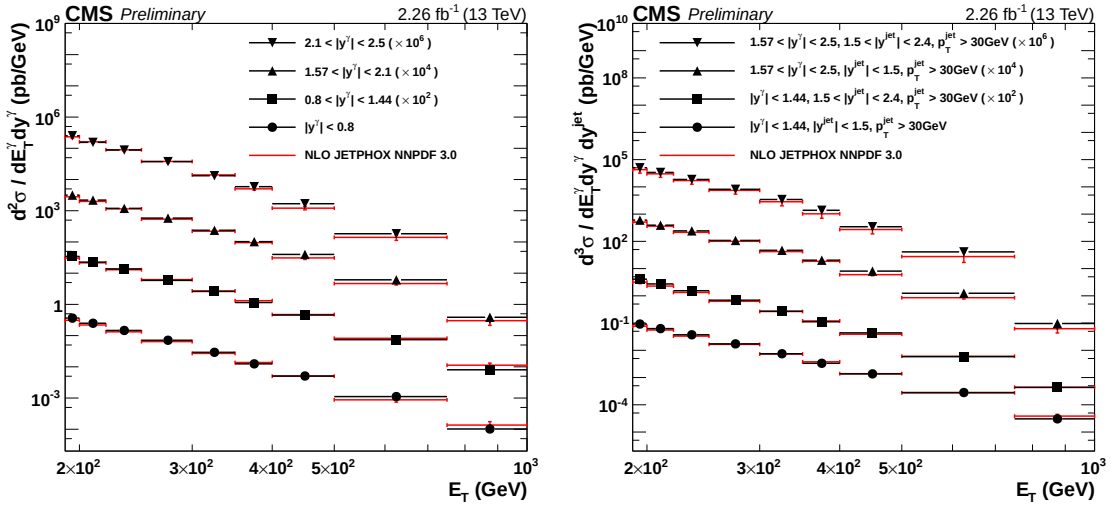

Figure 10: Inclusive photon (left) and photon+jet (right) differential cross sections as a function of E_{T}^{γ} compared to NLO theoretical predictions [24]

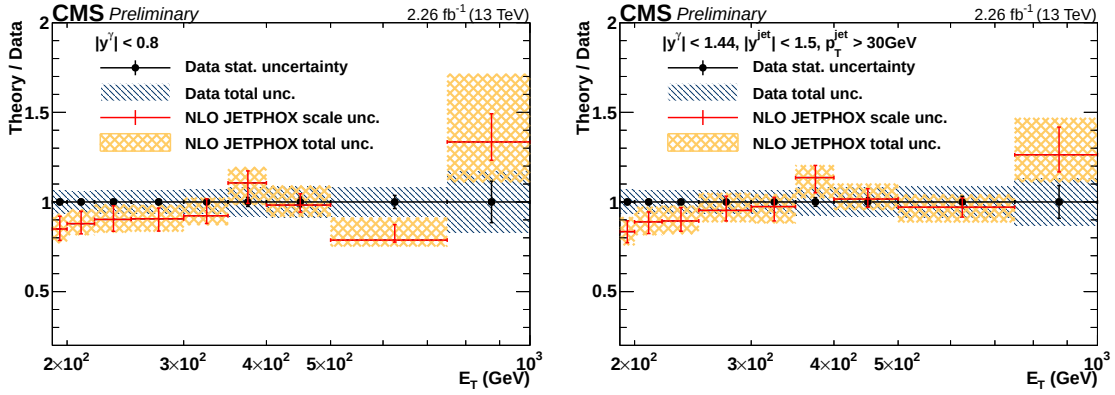

Figure 11: Ratio of the theoretical predictions to the data for inclusive photon (left) and photon+jet (right) differential cross sections as a function of E_{T}^{γ} [24]

4. Summary and conclusions

Tests of QCD in different regimes using top pair, multijet and photon production in pp collisions recorded by the ATLAS and CMS Collaborations at the LHC have been presented. The comparison of the data to theoretical predictions at fixed order in QCD yield generally good qualitative agreement, although in some regimes where resummation effects are important, such as in event shapes in multijet events, significant differences can be observed. Important parameters of the QCD Lagrangian such as the top quark mass or the strong coupling constant α_s have been determined from the top production data, and new constrains on the parton distribution functions have been extracted. Theoretical developments such as higher order calculations for photon production have been recently available, and will significantly reduce the theoretical uncertainties for further measurements.

References

[1] ATLAS Collaboration, "The ATLAS Experiment at the CERN Large Hadron Collider". JINST 3 (2008) S08003.

[2] CMS Collaboration, "The CMS experiment at the CERN LHC". JINST 3 (2008) S08004.

[3] ATLAS Collaboration, "Measurements of $t\bar{t}$ differential cross-sections of highly boosted top quarks decaying to all-hadronic final states in pp collisions at $\sqrt{s} = 13$ TeV using the ATLAS detector". Phys. Rev. D 98, 012003 (2018).

[4] M. Cacciari, G.P. Salam and G. Soyez. "The anti-k t jet clustering algorithm". JHEP 04 (2008) 063.

[5] ATLAS Collaboration, "Measurements of differential cross sections of top quark pair production in association with jets in pp collisions at $\sqrt{s} = 13$ TeV using the ATLAS detector". JHEP 10 (2018) 159.

[6] S. Alioli *et al.*, "A general framework for implementing NLO calculations in shower Monte Carlo programs: the POWHEG BOX". JHEP 06 (2010) 043.

[7] J. Alwall *et al.*, "The automated computation of tree-level and next-to-leading order differential cross sections, and their matching to parton shower simulations", JHEP 07 (2014) 079.

[8] T. Sjöstrand, S. Mrenna and P. Z. Skands, "A brief introduction to PYTHIA 8.1". Comput. Phys. Commun. 178 (2008) 852.

[9] M. Bähr *et al.*, "Herwig++ physics and manual". Eur. Phys. J. C 58 (2008) 639.

[10] T. Gleisberg *et al.*, "Event generation with SHERPA 1.1". JHEP 02 (2009) 007.

[11] CMS Collaboration, "Measurement of the $t\bar{t}$ production cross section, the top quark mass, and the strong coupling constant using dilepton events in pp collisions at $\sqrt{s} = 13$ TeV". Eur. Phys. J. C 79 (2019) 368.

[12] CMS Collaboration, "Measurements of $t\bar{t}$ differential cross sections in proton-proton collisions at $\sqrt{s} = 13$ TeV using events containing two leptons. JHEP 02 (2019) 149.

[13] CMS Collaboration, "Measurement of $t\bar{t}$ normalised multi-differential cross sections in pp collisions at $\sqrt{s} = 13$ TeV, and simultaneous determination of the strong coupling strength, top quark pole mass, and parton distribution functions". arXiv:1904.05237 [hep-ex]. z

[14] ATLAS Collaboration, "Properties of jet fragmentation using charged particles measured with the ATLAS detector in pp collisions at $\sqrt{s} = 13$ TeV". arXiv:1906.09254 [hep-ex].

[15] E.M. Metodiev and J. Thaler, "Jet Topics: Disentangling Quarks and Gluons at Colliders". Phys. Rev. Lett. 120, 241602 (2018).

[16] ATLAS Collaboration, "Properties of $g \to b\bar{b}$ at small opening angles in pp collisions with the ATLAS detector at $\sqrt{s} = 13$ TeV". Phys. Rev. D 99, 052004 (2019).

[17] M. Cacciari, G. P. Salam and G. Soyez, "The catchment area of jets". JHEP 04 (2008) 005.

[18] CMS Collaboration, "Event shape variables measured using multijet final states in proton-proton collisions at $\sqrt{s} = 13$ TeV". JHEP 12 (2018) 117.

[19] CMS Collaboration, "Azimuthal separation in nearly back-to-back jet topologies in inclusive 2- and 3-jet events in pp collisions at $\sqrt{s} = 13$ TeV". arXiv:1902.04374 [hep-ex].

[20] X. Chen *et al.*, "Isolated photon and photon+jet production at NNLO QCD accuracy". arXiv:1904.01044 [hep-ph].

[21] ATLAS Collaboration, "Measurement of the ratio of cross sections for inclusive isolated-photon production in pp collisions at $\sqrt{s} = 13$ and 8 TeV with the ATLAS detector". JHEP 04 (2019) 093.

[22] ATLAS Collaboration, "Measurement of the cross section for inclusive isolated-photon production in pp collisions at $\sqrt{s} = 13$ TeV using the ATLAS detector". Phys. Lett. B 770 (2017) 473.

[23] ATLAS Collaboration, "Measurement of the inclusive isolated prompt photon cross section in pp collisions at $\sqrt{s} = 8$ TeV with the ATLAS detector". JHEP 06 (2016) 005.

[24] CMS Collaboration, "Measurement of differential cross sections for inclusive isolated-photon and photon+jet production in proton-proton collisions at $\sqrt{s} = 13$ TeV". Eur. Phys. J. C 79 (2019) 20.

[25] P. Aurenche *et al.*, "A new critical study of photon production in hadronic collisions", Phys. Rev. D 73 (2006) 094007.

[26] S. Catani, M. Fontannaz, J. P. Guillet, and E. Pilon, "Cross section of isolated prompt photons in hadron-hadron collisions", JHEP 05 (2002) 028.

[27] Z. Belghobsi *et al.*, "Photon-jet correlations and constraints on fragmentation functions", Phys. Rev. D 79 (2009) 114024.